Received: 3 June 2024 | Revised: 28 June 2024 | Accepted: 3 July 2024

DOI: 10.1111/jace.20040

Journal of the American Ceramic Society

RAPID COMMUNICATION

Room-temperature bulk plasticity and tunable dislocation densities in $KTaO_3$

Xufei Fang[1,a,#] | **Jiawen Zhang**[2,#] | **Alexander Frisch**[1,a] | **Oliver Preuß**[3] | **Chukwudalu Okafor**[1,a] | **Martin Setvin**[4] | **Wenjun Lu**[2]

[1]Institute for Applied Materials, Karlsruhe Institute of Technology, Karlsruhe, Germany

[2]Department of Mechanical and Energy Engineering, Southern University of Science and Technology, Shenzhen, China

[3]Department of Materials and Earth Sciences, Technical University of Darmstadt, Darmstadt, Germany

[4]Department of Surface and Plasma Physics, Charles University, Praha, Czech Republic

Correspondence
Xufei Fang, Institute for Applied Materials, Karlsruhe Institute of Technology, 76131 Karlsruhe, Germany.
Email: xufei.fang@kit.edu

Wenjun Lu, Department of Mechanical and Energy Engineering, Southern University of Science and Technology, 518055 Shenzhen, China.
Email: luwj@sustech.edu.cn

Editor's Choice
The Editor-in-Chief recommends this outstanding article.

Funding information
European Research Council (ERC), Grant/Award Number: 101076167; Deutsche Forschungsgemeinschaft, Grant/Award Number: 510801687; DFG, Grant/Award Number: 414179371; Czech Science Foundation, Grant/Award Number: GACR 20–21727X; Shenzhen Science and Technology Program, Grant/Award Number: JCYJ20230807093416034; National Natural Science Foundation of China, Grant/Award Number: 52371110; Guangdong Basic and Applied Basic Research Foundation, Grant/Award Number: 2023A1515011510

Abstract

We report room-temperature bulk plasticity mediated by dislocations in single-crystal cubic potassium tantalate oxide ($KTaO_3$), contrasting the conventional knowledge that single-crystal $KTaO_3$ is susceptible to brittle fracture. A mechanics-based combinatorial experimental approach using cyclic Brinell indentation, scratching, and uniaxial bulk compression consistently demonstrates room-temperature dislocation plasticity in $KTaO_3$ from the mesoscale to the macroscale. This approach also delivers tunable dislocation densities and plastic zone size. Scanning transmission electron microscopy analysis underpins the activated slip system to be <110> $\{1\bar{1}0\}$. Given the growing significance of $KTaO_3$ as an emerging electronic oxide and the increasing interest in dislocations for tuning the physical properties of oxides, our findings are expected to trigger synergistic research interest in $KTaO_3$ with tunable dislocation densities.

KEYWORDS

bulk compression, cyclic deformation, dislocation, $KTaO_3$, scanning transmission electron microscopy

[#]These authors contribute equally to this work.

[a]Previously in the Department of Materials and Earth Sciences at the Technical University of Darmstadt where this work was initiated.

1 | INTRODUCTION

Ceramics are generally known for their brittleness at room temperature, primarily due to the lack of dislocation-mediated plasticity. Recent advancements have demonstrated room-temperature dislocation plasticity in various ceramic materials at small scales using techniques like nanoindentation[1–3] and nano-/micropillar compression.[4,5] These methods minimize flaw populations and favor plastic flow over cracking or suppress crack propagation through locally high compressive hydrostatic stress (as seen in nanoindentation with shallow depth) or by reducing the deformed volumes (in nano-/micropillar compression).

In contrast, ceramics that exhibit bulk and mesoscale plasticity under ambient conditions are relatively rare, despite their long research history. Alkali halide crystals, such as LiF, NaCl, and KCl, have been extensively studied for their dislocation mechanics since the 1950s. Classic studies by Johnston and Gilman on LiF single crystals have systematically explored dislocation multiplication, nucleation, and mobility through dislocation etch pit studies.[6–8] Similarly, NaCl crystals have been pivotal in understanding dislocation-based fracture toughness[9,10] and electro-plasticity as well as the charge of dislocations in ionic crystals.[11] Another notable group of ductile ceramics includes simple oxides with rock-salt structures, for instance, single-crystal MgO. Discovered to be plastically deformable in bulk compression[12,13] as early as in the late 1950s, MgO continues to be studied for its fundamental role in the Earth's lower mantle[14] and as a model system for understanding the elementary dislocation mechanics in oxides.[15]

Due to the wide bandgap of the aforementioned ductile crystals, their application in electronic devices is limited. Consequently, more attention has been directed towards other ductile semiconductors such as ZnS[16] and perovskite oxides. In 2001, Brunner et al.[17] reported the *surprising* discovery of room-temperature plasticity in $SrTiO_3$ (cubic structure) perovskite oxide, demonstrating a plastic strain up to ~7% under uniaxial bulk compression. Owing to its prototypical nature in condensed matter physics[18,19] and its role as a model electronic oxide, $SrTiO_3$ has been extensively studied thereafter for its dislocation plasticity, ranging from macroscale[20] and mesoscale[21,22] to nanoscale.[23–26] Later in 2016, Mark et al.[27] reported *unexpected* bulk plasticity in single-crystal $KNbO_3$, which is orthorhombic (peudo-cubic) at room temperature.[28] This finding in $KNbO_3$ was further confirmed by Höfling et al. in 2021[29] and Preuß et al. in 2023.[30] So far, $SrTiO_3$ and $KNbO_3$ have remained the only two perovskite oxides reported in the literature regarding room-temperature bulk plasticity.

In light of the increasing interest in using dislocations as one-dimensional line defects in ceramic oxides to harvest both functional and mechanical properties,[31,32] there is a pressing need to seek more room-temperature ductile ceramics as well as to engineer dislocations into such functional oxides for harnessing dislocation-tuned properties. Recently, we achieved this by developing an experimental toolbox for tuning dislocation densities and plastic zone sizes,[33] for example, in $SrTiO_3$. However, the pursuit of finding more room-temperature ductile ceramics remains largely unexplored so far. With the abundant techniques and experimental protocols recently established for room-temperature dislocation engineering,[33] we begin our quest to discover other ceramics that can be plastically deformed at room temperature at meso-/macroscale.

Here we report the third ductile perovskite oxide (potassium tantalate oxide, $KTaO_3$), independent of Khayr et al.,[34] on its room-temperature plasticity, with tunable dislocation densities and plastic zone size using a mechanics-based combinatorial experimental approach via cyclic Brinell indentation, scratching, and uniaxial bulk compression. $KTaO_3$ recently received much attention, owing to its potential for functional oxide electronics[35,36] and tunable ferroelectricity that is achieved through Nb doping.[37] These physical properties extend applications of $KTaO_3$ toward piezocatalysis, pyrocatalysis,[38] and photocatalysis.[39,40] Dislocations represent an additional degree of freedom that translates into all these applications, and it is therefore likely to spark more research interest in dislocation-tuned functional properties in $KTaO_3$.

2 | EXPERIMENTAL PROCEDURE

For cyclic Brinell indentation and scratching tests, a sample with a geometry of ~1×5×5 mm was used. The synthetic undoped single-crystal $KTaO_3$ sample was prepared by solidification from a nonstoichiometric melt in Oak Ridge National Laboratory. The tests were run on a universal hardness tester (Finotest; Karl-Frank GmbH), following the experimental procedure established by the current authors.[21,22] The indenter was mounted with a Brinell indenter with a diameter of 2.5 mm (hardened steel ball; Habu Hauck Prüftechnik GmbH) and a movable stage (Physik Instrumente GmbH & Co. KG). For both cyclic indentation and scratching tests, a dead weight of 1 kg was used. For scratching tests, a speed of 0.5 mm/s (lateral motion) was adopted. Additionally, silicone oil was used as a lubricant to reduce the indenter wear and to suppress sample crack formation. After mechanical deformation, the sample was cleaned with acetone and dried in air. The surface slip traces in the plastic zones were visualized using a laser confocal microscope (LEXT OLS4000;

Olympus IMS). Dark-field imaging mode was used on a Zeiss optical microscope (Zeiss Axio Imager2; Carl Zeiss AG) to exclude potential crack formation underneath the surface.

For uniaxial bulk compression, single-crystal samples (Hefei Single Crystal Material Technology) with a dimension of 3×3×6 mm were used. The long axis of the samples was aligned in the <001> direction. The samples were six-sided polished to mirror finish to minimize surface damage. Uniaxial compression was performed with a constant strain rate of 1.5×10^{-4} s^{-1} (MTS E45). The deformation images were collected in the VIC-gauge 2D software (Correlated Solution, Inc.). Before compression, two Al_2O_3 plates were placed on top and bottom of the $KTaO_3$ specimen to offer smoother contact surfaces.

To visualize the dislocation structures in the plastic zone, transmission electron microscopy (TEM) lamellae were lifted out along the scratching direction using a focused ion beam (FIB). The lamellae with a thickness of ~80 nm were prepared and thinned by a FIB (Helios Nanolab 600i, FEI). Microstructures of $KTaO_3$ including dislocations were characterized by a 200 kV-TEM (FEI Talos F200X G2, Thermo Fisher Scientific, USA) with STEM mode. The annular bright field-scanning transmission electron microscopy (ABF-STEM) images were collected with inner and outer semi-collection angles of 12–20 mrad.

3 | RESULTS AND ANALYSES

3.1 | Brinell indentation and scratching

Figure 1A–C demonstrates the surface plastic deformation after 1 cycle (1x) and 10 cycles (10x) Brinell indentation. The surface slip traces are aligned vertically and horizontally after 1x and 10x indentation (Figure 1A), and the slip trace number increases from 1x to 10x indentation (Figure 1B). The depth profiles of these two indentation imprints in Figure 1C (corresponding to the two yellow dashed lines in Figure 1A,B) indicate a maximum depth of ~120 nm after 1x and ~220 nm after 10x indentation. The plastic zone size in both cases has a diameter of ~150 μm, suggesting that the surface is nominally flat in the indented region.

In addition to the cyclic Brinell indentation test, cyclic scratching tests were performed using the same indenter. Figure 1D,E reveals an increase in the slip trace densities with the increasing scratching number from 1x to 10x. For scratching, each cycle is defined as one traversal. The maximum depth of the scratch tracks (Figure 1F, corresponding to the two yellow dashed lines in Figure 1D,E) was measured to increase from ~100 nm (1x) up to ~250 nm (10x). Different from the sink-in feature in the 1x scratching as well as the 1x and 10x indentation imprints, the 10x scratching depth profile exhibits two shoulders (pile-up, indicated by the two red arrows in Figure 1F). This pile-up was likely caused by the "plastic plowing" of the material by the spherical indenter during the back-and-forth cyclic scratching (scratching directions indicated by the yellow arrows in Figure 1E). This pile-up is strong evidence of good room-temperature plastic deformation of this material.

To rule out the possible cracking underneath the indentation imprints/scratch track, dark-field imaging mode (sensitive to under-surface cracks, featured as white contrasts) was used. No visible cracks were found up to 25 cycles of scratching. This observation is consistent with the results obtained on other ductile oxides (e.g., $SrTiO_3$[21,22]) at room temperature. Worth mentioning is that both the Brinell ball indentation and scratching test results in $KTaO_3$ closely resemble the slip trace features in $SrTiO_3$ with the same (001) surface being deformed. The plastic zone size is also almost identical for $KTaO_3$ observed here as in $SrTiO_3$[21] under the same loading conditions. Such similarities suggest that the lattice friction stress in $KTaO_3$ shall be sufficiently low to allow easy dislocation glide and multiplication at room temperature. Note that single-crystal $SrTiO_3$ was reported to plastically yield around 110–150 MPa during bulk compression along the [001] orientation (summarized literature results by Stich et al.[41]). If the deformation behavior is similar for these two perovskite oxides, then the yield strength of single-crystal $KTaO_3$ should be around the same range. To this end, further validation with uniaxial bulk compression was performed on $KTaO_3$ along the [001] direction.

3.2 | Uniaxial bulk compression

The engineering stress-strain curve in Figure 2A and the deformation process in Figure 2B demonstrate the bulk plastic deformation. Unlike the room-temperature bulk stress-strain curves in $SrTiO_3$[17,42] and $KNbO_3$,[27,29] here for $KTaO_3$ it exhibits an upper yield point and a lower yield point (indicated in Figure 2A). The upper yield point (Figure 2A) is σ_{y_up} = 274 MPa and the lower yield point is σ_{y_low} = 250 MPa. This load drop behavior is not uncommon for ceramics that undergo plastic deformation. For instance, similar yield behavior was reported in bulk compression of sapphire at high temperature[43] and discussed in single-crystal LiF at room temperature.[44] Due to the initially low mobile dislocation density in such ceramic crystals, dislocation multiplication was proposed to have caused such a stress drop instead of due to the unpinning of

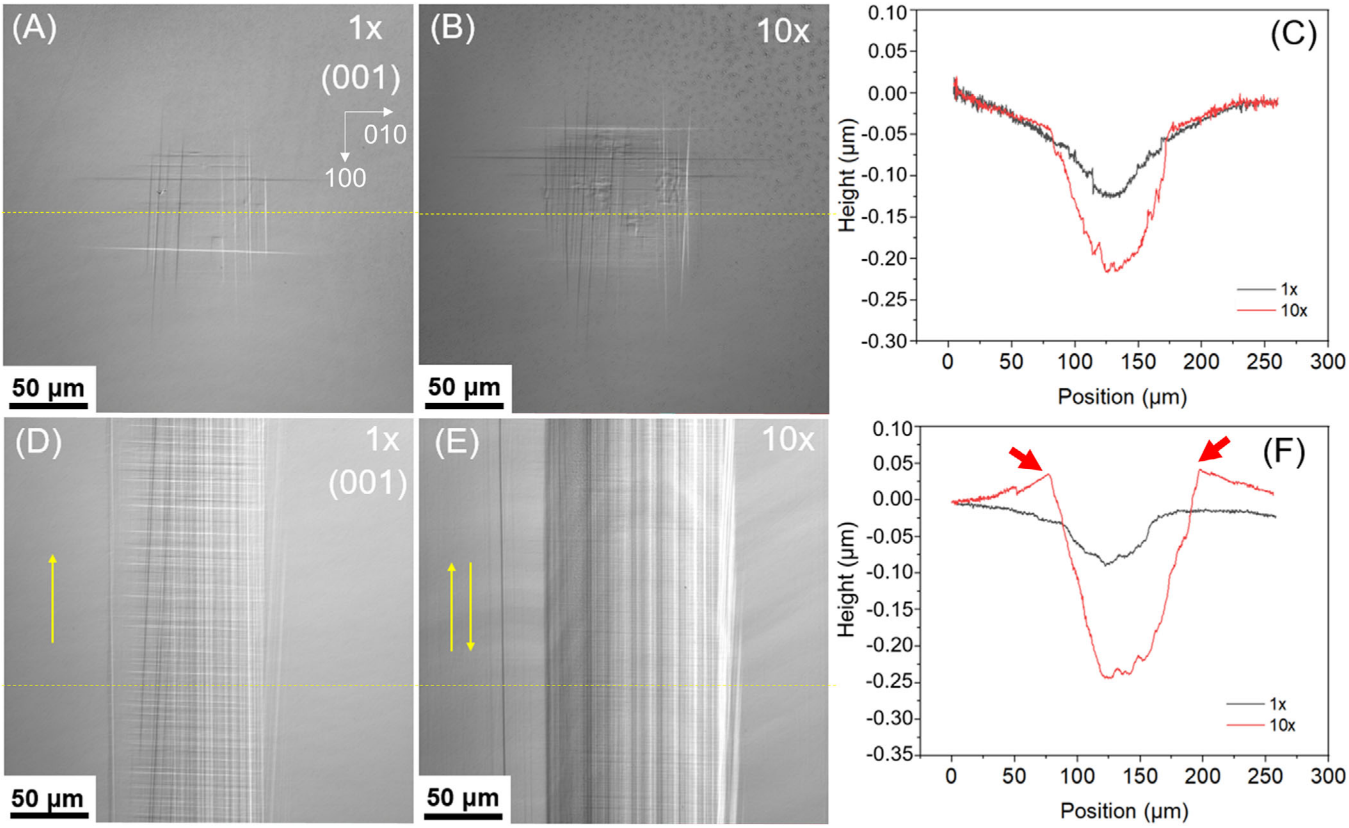

FIGURE 1 Laser microscope images featuring the plastic deformation on the (001) surface after Brinell ball indentation (A, B) and scratching (D, E). Note 1x and 10x stand for 1-cycle and 10-cycle deformation, respectively. The yellow arrows in (D, E) indicate the scratching direction. Depth profiles (C, F) corresponding to the yellow dashed lines were extracted, with the unperturbed sample surface corresponding to the zero point in the y-axis.

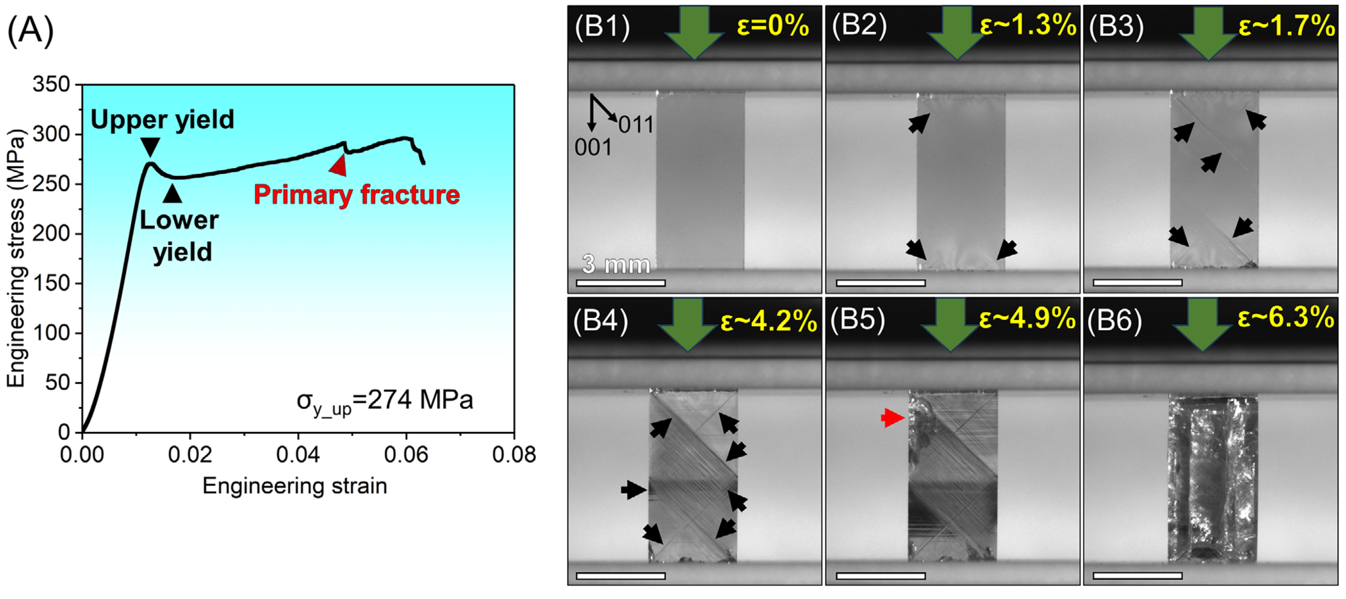

FIGURE 2 Bulk compression of single-crystal $KTaO_3$ along the <001> direction: (A) engineering stress-strain curve; (B1–B6) Screenshots of the in-situ bulk compression at different strains. The black arrows indicate the slip traces and the red arrow indicates the crack formation. The scale bar in (B1) is consistent for all six sub-figures.

a Cottrell cloud as in the case of α-iron, where dislocation pinning results from the impurities such as carbon.[45]

Following the upper yield point and then the lower yield point, the stress increased from 250 MPa (i.e., the lower yield point in Figure 2A) up to ~300 MPa, where another load drop was observed (red arrow in Figure 2A). On the one hand, the stress increase after the lower yield point indicates work hardening behavior, as evidenced by the increased number of slip traces (dark lines that lie 45° to the loading axis), indicated by the black arrows in Figure 2B3-B4. These slip traces confirm that the dislocation glide occurs on the {110} planes. On the other hand, the load drop (red arrow in Figure 2A) was found to correspond to the primary fracture event observed by the in-situ deformation (Figure 2B5, where the bright features on the top right corner indicate a main crack formed, see the red arrow). The deformed sample was captured (Figure 2B6, at a strain of ~6.3%) right before the sample shattered into pieces at a maximum strain of ~6.5%. Note the sample in Figure 2B6 is already full of cracks as reflected by the white contrast.

The observed yield stress during bulk compression agrees with the stress analysis using Hertzian contact for the Brinell ball indentation in Figure 1, as will be rationalized in the following. Consider that the post-mortem plastic zone imprint (Figure 1A) has a diameter of D = 150 μm, with the load of P = 1 kg (9.8 N), we estimate the mean pressure p_0 underneath the indenter to be ~555 MPa using the expression $p_0 = P/(\pi D^2/4)$.[46] The maximum shear stress (upon plastic yield) during spherical indentation can be calculated according to Swain & Lawn,[46] giving a value of about τ_{max} = 255 MPa (0.46p_0). Note that the critical resolved shear stress (τ_{CRSS}) in the current uniaxial bulk compression is half of the value of the yield strength (here we take the upper yield strength σ_{y_up} = 274 MPa in Figure 2A), giving τ_{CRSS} = 137 MPa. The estimation above is made on the Brinell indentation imprint, which is already in the plastic deformation regime. Consider that Hertzian contact theory is used for elastic deformation, the τ_{max} is expected to be larger than τ_{CRSS}. As both the τ_{max} and τ_{CRSS} are much smaller than the theoretical shear strength (~19 GPa for $KTaO_3$, estimated by $G/2\pi$, G is the shear modulus) for homogeneous dislocation nucleation, this suggests that the plastic deformation under the large Brinell indenter as well as the uniaxial bulk compression is mediated by dislocation multiplication and dislocation glide. It is thus expected that the lattice friction stress for dislocation glide in $KTaO_3$ at room temperature shall be close to τ_{CRSS} = 137 MPa (which is likely an upper bound). This value is higher but close to that in $SrTiO_3$ (~90 MPa[47]) and $KNbO_3$ (~30 MPa[27,29]).

3.3 | TEM characterization of dislocations

To directly prove that the dislocation densities in the plastic zone can be tuned via dislocation multiplication by increasing the number in the deformation cycles, we performed TEM analysis in the 1x and 10x scratched regions. As illustrated in Figure 3A, there are a few dislocations with long segments in the area of view after 1x scratching. These long segments are aligned on the {110} planes. This is consistent with the slip trace observation during bulk deformation (Figure 2B). After 10x scratching, the dislocation density increased dramatically and the dislocation lines were heavily tangled up with each other, where the dislocation density is estimated to be higher than $10^{14}/m^2$. Although the majority of the dislocations are still projected in the <110> directions, many short and curved dislocation segments are generated. These features are a result of the cyclic scratching, which strongly promotes dislocation multiplication and interaction. Such profuse dislocation multiplication significantly increases the dislocation plasticity, which is in line with the observation of the pile-up behavior after 10x Brinell ball scratching. Further analysis of the Burgers vector and the line vector of the dislocations suggest a Burgers vector of <110> and both edge and screw types of dislocations are generated. It is thus confirmed that $KTaO_3$ has the same slip system as in the case of $SrTiO_3$[18] and $KNbO_3$ (pseudo-cubic),[27] namely, the <110> $\{1\bar{1}0\}$ slip systems are activated at room temperature.

4 | DISCUSSION

Single-crystal $KTaO_3$ was reported to be very susceptible to brittle cleavage along the (001) surface.[48] Independent of the current work, Khayr et al.[34] studied the dislocation structural properties of plastically deformed $KTaO_3$ without direct visualization of the deformation features such as slip traces (Figures 1,2) and dislocation mesostructures (Figure 3). Here we present compelling evidence of room-temperature plasticity in single-crystal $KTaO_3$, with successful dislocation engineering at both the mesoscale and the bulk scale without inducing visible cracks. This crack suppression is attributed to the profuse dislocation multiplication and good dislocation mobility under the blunt spherical Brinell indenter, which proves to be more advantageous than pyramidal indenters such as Vickers indenter that is widely used for indentation fracture toughness evaluation in brittle solids.[49,50]

The choice of $KTaO_3$ was made based on its structural and atomic similarities to the other two ductile

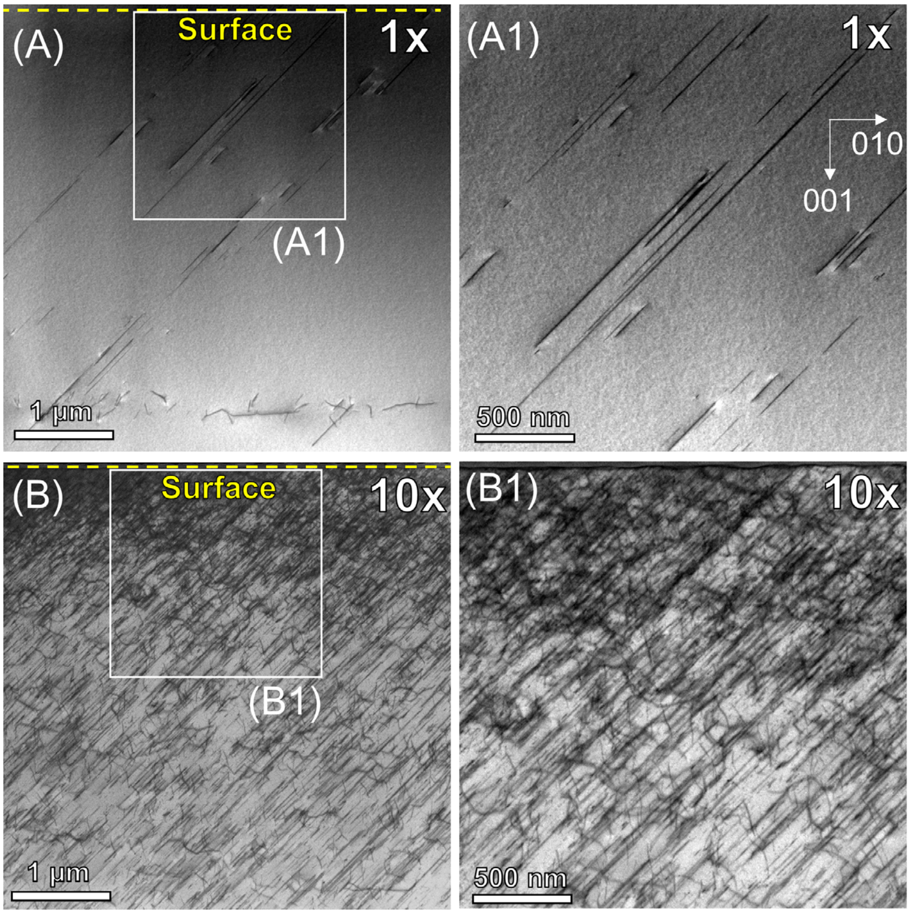

FIGURE 3 Visualization of dislocations (dark lines) in annular bright field-scanning transmission electron microscopy (ABF-STEM): (A) after 1x scratching; (B) after 10x scratching. The dislocation density is tunable depending on the number of cyclic scratching. The orientations in (A1) are consistent for all four sub-figures.

perovskite oxides $SrTiO_3$ and $KNbO_3$. $KTaO_3$ has a cubic structure at room temperature similar to $SrTiO_3$, also Ta and Nb have the same ionic radii of 0.64 Å (for +5 charge state and 6-fold coordination).[51] This led to our original hypothesis that $KTaO_3$ might also be ductile at room temperature, like $SrTiO_3$ and $KNbO_3$. At this stage, the underlying mechanisms for yielding such dislocation plasticity in $KaTiO_3$ remain unclear. Nevertheless, considering that $KTaO_3$, $SrTiO_3$, and $KNbO_3$ are very similar in crystal structure and much often used together for comparison in their physical properties,[35] it is likely that the dislocation mechanisms in these materials are similar, particularly concerning the dislocation core structure. For instance, TEM observations and atomistic simulations in $SrTiO_3$[52,53] as well as in $KNbO_3$[28] suggest that the dislocations are dissociated into partials, which facilitates good dislocation mobility at room temperature. To confirm if this is the case for $KTaO_3$, future work will involve high-resolution TEM characterization as well as molecular dynamics simulations in this direction.

It is worth noting that, due to the earlier discovery of room-temperature bulk dislocation plasticity and the simple dislocation introduction process in $SrTiO_3$, most of the dislocation-based functional and mechanical properties studies[54–56] have been reported using this model material. Now with the simple and efficient dislocation engineering demonstrated here in $KTaO_3$, and considering that $KTaO_3$ has been deemed as the “new kid on the spintronics block”,[35] it is expected that our finding will serve as a fundamental building block for upcoming versatile studies in $KTaO_3$ tuned by dislocations.

5 | CONCLUSION

We found that single-crystal $KTaO_3$ with a cubic structure can be plastically deformed at room temperature via bulk uniaxial compression, Brinell ball indentation, and scratching. The room-temperature slip systems in $KTaO_3$ are identified to be <110> $\{1\bar{1}0\}$, the same as those observed in $SrTiO_3$ and $KNbO_3$ deformed at room temperature.

For the single crystals compressed along the <001> direction in this work, the bulk yield strength of $KTaO_3$ was ~274 MPa, and the critical resolved shear stress is estimated to be ~137 MPa (likely the upper bound) to move the dislocations. Unlike the discrete slip bands generated during bulk compression, the Brinell ball indentation and scratching generate continuous plastic zones extending up to hundreds of micrometers with dislocation densities exceeding ~$10^{14}/m^2$ after 10-cycle scratching. It remains an open question at this stage to pinpoint the fundamental mechanisms responsible for the room-temperature dislocation plasticity in $KTaO_3$. Our findings are expected to open new avenues to investigate dislocation-tuned mechanical and functional properties in $KTaO_3$.

ACKNOWLEDGMENTS

X. Fang and A. Frisch acknowledge the European Research Council (ERC) under grant number 101076167 (MECERDIS) for supporting the research. Views and opinions expressed are, however, those of the authors only and do not necessarily reflect those of the European Union or the European Research Council. Neither the European Union nor the granting authority can be held responsible for them. C. Okafor acknowledges the financial support by the Deutsche Forschungsgemeinschaft (DFG, grant No. 510801687). O. Preuß thanks the DFG for the funding (grant No. 414179371). M. Setvin acknowledges the support from the Czech Science Foundation, project GACR 20–21727X. W. Lu is supported by the Shenzhen Science and Technology Program (grant number JCYJ20230807093416034), the National Natural Science Foundation of China (grant number 52371110), and the Guangdong Basic and Applied Basic Research Foundation (grant number 2023A1515011510). The authors acknowledge the use of the facilities at the Southern University of Science and Technology Core Research Facility. M. Setvin and X. Fang would like to thank L. A. Boatner at Oak Ridge National Laboratory for providing the $KTaO_3$ crystal for the indentation tests. We thank Prof. Rödel at TU Darmstadt for the discussion.

Open access funding enabled and organized by Projekt DEAL.

ORCID

Xufei Fang https://orcid.org/0000-0002-3887-0111

REFERENCES

1. Basu S, Barsoum MW. Deformation micromechanisms of ZnO single crystals as determined from spherical nanoindentation stress–strain curves. J Mater Res. 2007;22(9):2470–77.
2. Page TF, Oliver WC, McHargue CJ. The deformation behavior of ceramic crystals subjected to very low load (nano)indentations. J Mater Res. 2011;7(2):450–73.
3. Fang X, Bishara H, Ding K, Tsybenko H, Porz L, Höfling M, et al. Nanoindentation pop-in in oxides at room temperature: dislocation activation or crack formation? J Am Ceram Soc. 2021;104:4728–41.
4. Korte-Kerzel S. Microcompression of brittle and anisotropic crystals: recent advances and current challenges in studying plasticity in hard materials. MRS Commun. 2017;7(2):109–20.
5. Fujikane M, Nagao S, Chrobak D, Yokogawa T, Nowak R. Room-temperature plasticity of a nanosized GaN crystal. Nano Lett. 2021;21(15):6425–31.
6. Gilman JJ, Johnston WG. Observations of dislocation glide and climb in lithium fluoride crystals. J Appl Phys. 1956;27(9):1018–22.
7. Johnston WG, Gilman JJ. Dislocation velocities, dislocation densities, and plastic flow in lithium fluoride crystals. J Appl Phys. 1959;30(2):129–44.
8. Johnston WG, Gilman JJ. Dislocation multiplication in lithium fluoride crystals. J Appl Phys. 1960;31(4):632–43.
9. Higashida K, Narita N, Matsunaga K. Effect of dislocation activities on crack extension in ionic crystals. Mater Sci Eng, A. 1994;176:147–53.
10. Higashida K, Narita N, Matsunaga K, Onodera R. Effects of low energy dislocation structures on crack tip shielding in ionic crystals. Phys Stat Sol A. 1995;149:429–43.
11. Whitworth RW. Charged dislocations in ionic crystals. Adv Phys. 1975;24(2):203–304.
12. Gorum AE, Parker ER, Pask JA. Effect of surface conditions on room-temperature ductility of ionic crystals. J Am Ceram Soc. 1958;41(5):161–64.
13. Stokes RJ, Johnston TL, Li CH. Crack formation in magnesium oxide single crystals. Philos Mag. 1958;3(31):718–25.
14. Cordier P, Amodeo J, Carrez P. Modelling the rheology of MgO under Earth's mantle pressure, temperature and strain rates. Nature. 2012;481(7380):177–80.
15. Gaillard Y, Tromas C, Woirgard J. Quantitative analysis of dislocation pile-ups nucleated during nanoindentation in MgO. Acta Mater. 2006;54(5):1409–17.
16. Oshima Y, Nakamura A, Matsunaga K. Extraordinary plasticity of an inorganic semiconductor in darkness. Science. 2018;360:772–74.
17. Brunner D, Taeri-Baghbadrani S, Sigle W, Rühle M. Surprising results of a study on the plasticity in strontium titanate. J Am Ceram Soc. 2001;84(5):1161–63.
18. Gumbsch P, Taeri-Baghbadrani S, Brunner D, Sigle W, Ruhle M. Plasticity and an inverse brittle-to-ductile transition in strontium titanate. Phys Rev Lett. 2001;87(8):085505.
19. Gao P, Yang S, Ishikawa R, Li N, Feng B, Kumamoto A, et al. Atomic-scale measurement of flexoelectric polarization at $SrTiO_3$ dislocations. Phys Rev Lett. 2018;120(26):267601.
20. Taeri S, Brunner D, Sigle W, Rühle M. Deformation behaviour of strontium titanate between room temperature and 1800 K under ambient pressure. Int J Mater Res. 2004;95(6):433–46.
21. Okafor C, Ding K, Zhou X, Durst K, Rödel J, Fang X. Mechanical tailoring of dislocation densities in $SrTiO_3$ at room temperature. J Am Ceram Soc. 2022;105:2399–402.
22. Fang X, Preuß O, Breckner P, Zhang J, Lu W. Engineering dislocation-rich plastic zones in ceramics via room-temperature scratching. J Am Ceram Soc. 2023;106:4540–45.

23. Javaid F, Bruder E, Durst K. Indentation size effect and dislocation structure evolution in (001) oriented $SrTiO_3$ Berkovich indentations: HR-EBSD and etch-pit analysis. Acta Mater. 2017;139:1–10.
24. Javaid F, Stukowski A, Durst K. 3D Dislocation structure evolution in strontium titanate: spherical indentation experiments and MD simulations. J Am Ceram Soc. 2017;100(3):1134–45.
25. Fang X, Ding K, Janocha S, Minnert C, Rheinheimer W, Frömling T, et al. Nanoscale to microscale reversal in room-temperature plasticity in $SrTiO_3$ by tuning defect concentration. Scr Mater. 2020;188:228–32.
26. Fang X, Ding K, Minnert C, Nakamura A, Durst K. Dislocation-based crack initiation and propagation in single-crystal $SrTiO_3$. J Mater Sci. 2021;56:5479–92.
27. Mark AF, Castillo-Rodriguez M, Sigle W. Unexpected plasticity of potassium niobate during compression between room temperature and 900°C. J Eur Ceram Soc. 2016;36(11):2781–93.
28. Hirel P, Mark AF, Castillo-Rodriguez M, Sigle W, Mrovec M, Elsässer C. Theoretical and experimental study of the core structure and mobility of dislocations and their influence on the ferroelectric polarization in perovskite $KNbO_3$. Phys Rev B. 2015;92(21):214101.
29. Hoefling M, Trapp M, Porz L, Ursic H, Bruder E, Kleebe H-J, et al. Large plastic deformability of bulk ferroelectric $KNbO_3$ single crystals. J Eur Ceram Soc. 2021;41:4098–107.
30. Preuß O, Bruder E, Lu W, Zhuo F, Minnert C, Zhang J, et al. Dislocation toughening in single-crystal $KNbO_3$. J Am Ceram Soc. 2023;106:4371–81.
31. Ikuhara Y. Nanowire design by dislocation technology. Prog Mater Sci. 2009;54(6):770–91.
32. Fang X, Nakamura A, Rödel J. Deform to perform: dislocation-tuned properties of ceramics. Am Ceram Soc Bull. 2023;102(5):24–29.
33. Fang X. Mechanical tailoring of dislocations in ceramics at room temperature: a perspective. J Am Ceram Soc. 2024;107(3):1425–47.
34. Khayr I, Hameed S, Budić J, He X, Spieker R, Najev A, et al. Structural properties of plastically deformed $SrTiO_3$ and $KTaO_3$. arXiv. 2024. https://doi.org/10.48550/arXiv.2405.13249
35. Gupta A, Silotia H, Kumari A, Dumen M, Goyal S, Tomar R, et al. Chakraverty, KTaO3 – the new kid on the spintronics block. Adv Mater. 2022, 34(9):e2106481.
36. Vicente-Arche LM, Brehin J, Varotto S, Cosset-Cheneau M, Mallik S, Salazar R, et al. Spin-charge interconversion in $KTaO_3$ 2D electron gases. Adv Mater. 2021;33(43):e2102102.
37. Toulouse J, Wang XM, Boatner LA. Elastic anomalies at the cubic-tetragonal transition in KTN. Solid State Commun. 1988;68:353–56.
38. Wang M, Wang B, Huang F, Lin Z. Enabling PIEZOpotential in PIEZOelectric semiconductors for enhanced catalytic activities. Angew Chem. 2019;58(23):7526–36.
39. Grabowska E. Selected perovskite oxides: Characterization, preparation and photocatalytic properties—a review. Appl Catal B. 2016;186:97–126.
40. Kakekhani A, Ismail-Beigi S, Altman EI. Ferroelectrics: A pathway to switchable surface chemistry and catalysis. Surf Sci. 2016;650:302–16.
41. Stich S, Ding K, Muhammad QK, Porz L, Minnert C, Rheinheimer W, et al. Room-temperature dislocation plasticity in $SrTiO_3$ tuned by defect chemistry. J Am Ceram Soc. 2022;105:1318–29.
42. Brunner D. Low-temperature plasticity and flow-stress behaviour of strontium titanate single crystals. Acta Mater. 2006;54(19):4999–5011.
43. Firestone RF, Heuer AH. Yield point of sapphire, J Am Ceram Soc. 2006;56(3):136–39.
44. Gilman JJ, Johnston WG. Behavior of individual dislocations in strain-hardened LiF crystals. J Appl Phys. 1960;31(4):687–692.
45. Cottrell AH, Bilby BA. Dislocation theory of yielding and strain ageing of iron. Proc Phys Soc Sect A. 1949:49–62.
46. Swain MV, Lawn BR. A study of dislocation arrays at spherical indentations in LiF as a function of indentation stress and strain. Phys Stat Sol. 1969;35:909–23.
47. Javaid F, Johanns KE, Patterson EA, Durst K. Temperature dependence of indentation size effect, dislocation pile-ups, and lattice friction in (001) strontium titanate. J Am Ceram Soc. 2018;101(1):356–64.
48. Setvin M, Reticcioli M, Poelzleitner F, Hulva J, Schmid M, Boatner LA, et al. Polarity compensation mechanisms on the perovskite surface $KTaO_3$ (001). Science. 2018;359:572–75.
49. Anstis GR, Chantikul P, Lawn BR, Marshall DB. A critical evaluation of indentation techniques for measuring fracture toughness: I, direct crack measurements. J Am Ceram Soc. 1981;64(9):533–38.
50. Lee JH, Gao YF, Johanns KE, Pharr GM. Cohesive interface simulations of indentation cracking as a fracture toughness measurement method for brittle materials. Acta Mater. 2012;60(15):5448–67.
51. Shannon RD. Revised effective ionic radii and systematic studies of interatomic distances in halides and chalcogenides. Acta Cryst A. 1976;32:751–67.
52. Matsunaga T, Saka H. Transmission electron microscopy of dislocations in $SrTiO_3$. Philos Mag Lett. 2000;80(9):597–604.
53. Klomp AJ, Porz L, Albe K. The nature and motion of deformation-induced dislocations in $SrTiO_3$: Insights from atomistic simulations. Acta Mater. 2023;242:118404.
54. Kissel M, Porz L, Frömling T, Nakamura A, Rödel J, Alexe M. Enhanced photoconductivity at dislocations in $SrTiO_3$. Adv Mater. 2022:2203032.
55. Hameed S, Pelc D, Anderson ZW, Klein A, Spieker RJ, Yue L, et al. Enhanced superconductivity and ferroelectric quantum criticality in plastically deformed strontium titanate. Nat Mater. 2022;21:54–61.
56. Szot K, Speier W, Bihlmayer G, Waser R. Switching the electrical resistance of individual dislocations in single-crystalline $SrTiO_3$. Nat Mater. 2006;5(4):312–20.

How to cite this article: Fang X, Zhang J, Frisch A, Preuß O, Okafor C, Setvin M, et al. Room-temperature bulk plasticity and tunable dislocation densities in $KTaO_3$. J Am Ceram Soc. 2024;107:7054–61. https://doi.org/10.1111/jace.20040